Biometals (2008) 21:635–648
DOI 10.1007/s10534-008-9149-4

Tandem heterocyclization domains in a nonribosomal peptide synthetase essential for siderophore biosynthesis in *Vibrio anguillarum*

Manuela Di Lorenzo · Michiel Stork · Hiroaki Naka · Marcelo E. Tolmasky · Jorge H. Crosa

Received: 15 May 2008 / Accepted: 27 May 2008 / Published online: 13 June 2008

Abstract Anguibactin, the siderophore produced by *Vibrio anguillarum* 775, is synthesized via a nonribosomal peptide synthetase (NRPS) mechanism. Most of the genes required for anguibactin biosynthesis are harbored by the pJM1 plasmid. Complete sequencing of this plasmid identified an *orf* encoding a 108 kDa predicted protein, AngN. In this work we show that AngN is essential for anguibactin biosynthesis and possesses two domains with homology to cyclization (Cy) domains of NRPSs. Substitution by alanine of the aspartic acid residues within a conserved motif of either Cy1 or Cy2 domain demonstrated the importance of these two domains in AngN function during siderophore biosynthesis. Site-directed mutations in both domains (D133A/D575A and D138A/D580A) resulted in anguibactin-deficient phenotypes while mutations in each domain did not abolish siderophore production but caused a reduction in the amounts produced. The mutations D133A/D575A and D138A/D580A also resulted as expected in a dramatic attenuation of the virulence of *V. anguillarum* 775 highlighting the importance of this gene for the biosynthesis of anguibactin within the vertebrate host. Regulation of the *angN* gene follows the patterns observed at the iron transport-biosynthesis promoter with *angN* transcription repressed in the presence of iron and enhanced by AngR and trans-acting factor (TAF) under iron limitation.

Keywords Iron · Siderophore · Nonribosomal peptide synthetase · Heterocyclization domain

M. Di Lorenzo (✉) · M. Stork · H. Naka · J. H. Crosa
Department of Molecular Microbiology and Immunology, Oregon Health & Science University, Portland, OR 97239-3098, USA
e-mail: m.dilorenzo@nioo.knaw.nl

M. Di Lorenzo
Department of Microbial Wetland Ecology, Netherlands Institute of Ecology, Nieuwersluis, The Netherlands

M. Stork
Department of Molecular Microbiology, Utrecht University, Utrecht, The Netherlands

M. E. Tolmasky
Department of Biological Science, California State University–Fullerton, Fullerton, CA, USA

Introduction

The possession of specialized iron transport systems is crucial for bacteria to override the iron limitation imposed by the host or the environment (Braun and Killmann 1999; Wandersman and Delepelaire 2004). Pathogenic bacteria have evolved systems, such as siderophores, to scavenge ferric iron from the iron-binding proteins of the host (Ratledge 2007). Peptide siderophores are in general low molecular-weight iron chelators that are synthesized by proteins belonging to the nonribosomal peptide synthetase (NRPS) family (Crosa and Walsh 2002; Miethke and

Marahiel 2007). NRPSs catalyze the formation of a wide variety of peptides, such as antibiotics and siderophores, in the absence of an RNA template (Finking and Marahiel 2004; von Dohren et al. 1999; Walsh 2004). These multimodular enzymes work as an enzymatic assembly line in which the order of the modules determines the order of the amino acids in the peptide (Fischbach and Walsh 2006; Marahiel et al. 1997). Each module contains the complete information for an elongation step combining the catalytic functions for the activation of the substrate amino acid (adenylation domain, A), the tethering of the corresponding adenylate to the enzyme-bound 4′-phosphopantetheinyl (4′-PP) cofactor (peptidyl carrier protein domain, PCP) and the formation of the peptide bond by the condensation domain, C (Keating and Walsh 1999; Marahiel et al. 1997; von Dohren et al. 1999). In some cases the condensation steps can also be catalyzed by a specialized condensation domain, the cyclization domain (Cy) that converts specific amino acids such as cysteine and threonine to their cyclic derivatives, thiazoline and oxazoline respectively, in the process of peptide bond formation (Marshall et al. 2001; Miller and Walsh 2001; Quadri et al. 1999; Walsh et al. 2001).

The bacterial fish pathogen *Vibrio anguillarum* is the causative agent of vibriosis, a highly fatal hemorrhagic septicemic disease in salmonids and other fish including eels (Actis et al. 1999). Many pathogenic strains of *V. anguillarum* possess a virulence plasmid that encodes an iron-sequestering system that includes a 348 Da siderophore, anguibactin (*ω-N*-hydroxy-*ω-N*((2′-(2″,3″-dihydroxyphenyl)thiazolin-4′-yl)carboxy) histamine), and a transport protein system for the binding and transport of iron as a complex with the siderophore anguibactin into the cell cytosol (Actis et al. 1986, 1988). The sequence of the 65 kilobase (kb) virulence plasmid pJM1 of *V. anguillarum* strain 775 has been completed (Di Lorenzo et al. 2003) and revealed that most of the proteins proposed to be involved in anguibactin biosynthesis are encoded by genes on the plasmid. Interestingly, the chromosome harbors redundant copies of genes encoding proteins for the biosynthesis of the anguibactin precursor 2,3-dihydroxybenzoic acid (DHBA) and anguibactin itself (Alice et al. 2005; Naka et al. 2008).

Several of the anguibactin biosynthetic proteins are part of the NRPS family (Di Lorenzo et al. 2004; Welch et al. 2000; Wertheimer et al. 1999) and one of these proteins, AngR, has also regulatory properties. AngR acts as a positive regulator of the *fatDCBAangRT* operon (Wertheimer et al. 1999); expression from this operon is also enhanced by TAF, an additional regulator encoded in a region of the virulence plasmid noncontiguous to the *fatDCBAangRT* operon (Tolmasky et al. 1988).

In this work we describe one of the genes harbored by the virulence plasmid pJM1, that encodes a putative NRPS, AngN. AngN shows an unusual domain organization for an NRPS with only two cyclization domains in tandem. Transposon insertions in the *angN* gene resulted in anguibactin-deficient mutants (Tolmasky et al. 1988). Our results demonstrate the essential role played by AngN and its cyclization domains in anguibactin biosynthesis.

Materials and methods

Bacterial strains and plasmids

Bacterial strains and plasmids used in this study are described in Table 1. *V. anguillarum* was grown at 25°C in either trypticase soy broth or agar supplemented with 1% NaCl, TSBS and TSAS respectively. To determine iron uptake characteristics, the strains were grown in M9 minimal medium (Sambrook and Russell 2001) supplemented with 0.2% Casamino acid, 1% NaCl, the appropriate antibiotics and either various concentrations of ethylenediamine-di-(*o*-hydroxyphenyl acetic acid) (EDDA) for iron-limiting conditions or 4 μg/ml ferric ammonium citrate for iron rich conditions. Antibiotic concentrations used for *V. anguillarum* were ampicillin (Ap) 1 mg/ml, tetracycline (Tc) 2.5 μg/ml, rifampicin (Rif) 100 μg/ml, chloramphenicol (Cm) 10–15 μg/ml and gentamicin (Gm) 10 μg/ml.

Escherichia coli strains were grown in Luria-Bertani (LB) medium in the presence of the appropriate antibiotics. Antibiotic concentrations used for *E. coli* were Ap 100 μg/ml, Tc 10 μg/ml, Cm 30 μg/ml, Gm 10 μg/ml and trimethropim (Tp) 10 μg/ml.

General methods

Plasmid DNA preparations were performed using the alkaline lysis method (Birnboim and Doly 1979). Restriction endonuclease digestion of DNA was

Table 1 Strains and plasmids used in this study

Bacterial strains	Genotype and relevant characteristics	Source or reference
Vibrio anguillarum 775 (pJM1)	Wild type	Crosa et al. (1980)
Vibrio anguillarum CC9-16(pJHC9-16)	Anguibactin-deficient, iron transport-proficient	Walter et al. (1983)
Vibrio anguillarum CC9-8(pJHC9-8)	Anguibactin-deficient, iron transport-deficient	Walter et al. (1983)
Vibrio anguillarum 775(pJM1-120)	775 carrying pJM1 with Tn*3*::Ho-Ho1 insertion in *angN*	This study
Vibrio anguillarum 775(pJM1-4)	775 carrying pJM1 with Tn*3*::Ho-Ho1 insertion in *angR*	Laboratory collection
Vibrio anguillarum H775-3	Plasmidless derivative of 775	Crosa et al. (1980)
Vibrio anguillarum H775-3(pJHC-T2612)	Plasmidless derivative of 775 carrying pJHC-T2612 (TAF^-)	Tolmasky et al. (1988)
Escherichia coli XL1 blue	*recA1, endA1,gyrA46, thi,hsdR17, supE44, relA,* *lac*F′ [*proAB*$^+$, *lacI*^{q}, *lacZΔM15* Tn*10* (Tet^r)]	Stratagene
Escherichia coli HB101	*supE44 hsd20* (r^{-B} m^{-B}) *recA13 ara-14 proA2 lacY1 galK2 rpsL20 xyl-5 mtl-1*	Boyer and Roulland-Dussoix (1969)

Plasmids	Relevant characteristics	Source or reference
pJM1	Indigenous plasmid in strain 775	Crosa et al. (1980)
pJHC-T2612	Recombinant clone carrying a 24 kb region of pJM1 cloned in pVK102, Tc^r	Tolmasky et al.(1988)
pJHC-T2612#120	pJHC-T2612 with a Tn*3*::Ho-Ho1 insertion in *angN,* Tc^r,Ap^r	Tolmasky et al. (1988)
pJHC9-8	pJM1 derivative carrying only the TAF region	Tolmasky et al. (1988)
pJHC9-16	pJM1 derivative carrying TAF and transport genes,	Tolmasky et al. (1988)
pPH1JI	Plasmid with RP4 *ori*, incompatible with pJHC-T2612, Gm^r	Hirsch and Beringer (1984)
pRK2073	Helper plasmid for conjugation, Tp^r, Tra^+	Figurski and Helinski (1979)
pBluescript SK^+	Cloning vector, Ap^r	Stratagene
pCR®-BluntII-TOPO®	Cloning vector, Km^r	Invitrogen
pBR325	Cloning vector, Tc^r, Cm^r, Ap^r	Bolivar (1978)
pBR325-M200	Cloning vector derived from pBR325, Tc^r, Cm^r, Ap^s	Di Lorenzo et al. (2004)
pTL61T	*lacZ* reporter vector, Ap^r	Linn and St Pierre (1990)
pMDL6	3.2 kb PCR fragment from pJM1 containing the *angN* gene cloned in pCR®-BluntII-TOPO®	This study
pMDL6-D133A	pMDL6 with mutation D133A in Cy_1 domain	This study
pMDL6-D138A	pMDL6 with mutation D138A in Cy_1 domain	This study
pMDL6-D575A	pMDL6 with mutation D575A in Cy_2 domain	This study
pMDL6-D580A	pMDL6 with mutation D580A in Cy_2 domain	This study
pMDL6-D133A/D575A	pMDL6 with mutation D133A in Cy_1 domain and D575A in Cy_2 domain	This study
pMDL6-D138A/D580A	pMDL6 with mutation D138A in Cy_1 domain and D580A in Cy_2 domain	This study
pMDL30	*Cla*I-*Bam*HI fragment from pMDL6 cloned in pBR325-M200	This study
pCy_1D_1-D133A	*Cla*I-*Bam*HI fragment from pMDL6-D133A cloned in pBR325-M200	This study

Table 1 continued

Plasmids	Relevant characteristics	Source or reference
pCy_1D_2-D138A	*Cla*I-*Bam*HI fragment from pMDL6-D138A cloned in pBR325-M200	This study
pCy_2D_1-D575A	*Cla*I-*Bam*HI fragment from pMDL6-D575A cloned in pBR325-M200	This study
pCy_2D_2-D580A	*Cla*I-*Bam*HI fragment from pMDL6-D580A cloned in pBR325-M200	This study
$pCy_{1/2}D_1$-D133A/D575A	*Cla*I-*Bam*HI fragment from pMDL6-D133A/D575A cloned in pBR325-M200	This study
$pCy_{1/2}D_2$-D138A/D580A	*Cla*I-*Bam*HI fragment from pMDL6-D138A/D580A cloned in pBR325-M200	This study
pCRII-P*angN*	350 bp PCR fragment from pJM1 containing the upstream region of the *angN* gene cloned in pCR®-BluntII-TOPO®	This study
pHNN-2	*Xho*I-*Pst*I fragment from pCRII-P*angN* cloned in pTL61T	This study
pSC50	125 bp *Sau*3AI fragment of the *fatB* gene cloned in pBluescript SK^+	Laboratory collection
pQSH6	415 bp *Sal*I-*Cla*I fragment of the *aroC* gene cloned in pBluescript SK^+	Di Lorenzo et al.(2004)

performed under the conditions recommended by the supplier (Invitrogen, Roche, NEB). Transformations in the *E. coli* strains HB101 and XL1 blue and other cloning strategies were performed according to standard protocols (Sambrook and Russell 2001). Plasmids were transferred from *E. coli* to *V. anguillarum* by conjugation as previously described (Tolmasky et al. 1988).

The Wizard® Plus SV Minipreps (Promega) and Qiaprep® Spin Miniprep Kit (Qiagen) were used to generate sequence quality plasmid DNA. DNA sequencing reactions were carried out by the OHSU-MMI Research Core Facility (http://www.ohsu.edu/core) using a model 377 Applied Biosystems Inc. automated fluorescence sequencer. Sequencing primers were designed using Oligo 6.8® primer analysis software and purchased from the OHSU-MMI Research Core Facility (http://www.ohsu.edu/core) and Invitrogen. DNA and protein sequence analysis were carried out at the NCBI using the BLAST network service (Altschul et al. 1990).

Mobilization of the *angN* mutation #120 from pJHC-T2612 to the pJM1 plasmid

To generate strain 775(pJM1-120), plasmid pJHC-T2612#120 was transferred to *V. anguillarum* 775 by conjugation. In a second conjugation, plasmid pPH1JI, whose origin of replication is incompatible with the replicon of pJHC-T2612#120, was transferred to the strain obtained from the first conjugation. By plating in the presence of Gm (the resistance marker of pPH1JI) and Ap (the resistance gene harbored by the Tn*3*::HoHo1 transposon), it was possible to select for those cells in which the *angN* gene with the Tn*3*::HoHo1 insertion had replaced the wild type gene on the pJM1 plasmid. The loss of pJHC-T2612 was confirmed by Southern blot hybridization using the pVK102 vector sequence for probing (data not shown). The Tn*3*::HoHo1 transposon harbors a mutation in the transposase gene that prevents transposition to occur to other locations on the plasmid or in the chromosome.

Construction of the complementing clone

A 3.2 kb fragment containing the *angN* gene was amplified by PCR using the *angN*-F and the *angN*-*Bam*HIR primers (Table 2) and pJM1 as a template. Reactions consisted of 2 min at 95°C followed by 30 cycles of 1 min at 95°C, 1 min at 53°C, and 4 min at 72°C followed by a single cycle at 72°C for 10 min. The PCR product was cloned in the pCR®-BluntII-TOPO® vector using the Zero Blunt® TOPO® PCR

Table 2 DNA primers used in this study

Primer name	Nucleotide sequence[a]
angN-F	5′-ACGACGATTGATGGGTGTAGC-3′
*angN-Bam*HIR	5′-TTGTATTCACTAT*GG*ATCCTTGC-3′
D133A-F	5′-CGCTTACATATTGATAGCG*C*TATGATTGCTATTGACCCAG-3′
D133A-R	5′-CTGGGTCAATAGCAATCATA*G*CGCTATCAATATGTAAGCG-3′
D138A-F	5′-CGATATGATTGCTATTG*C*CCCAGATAGTTGCCGAG-3′
D138A-R	5′-CTCGGCAACTATCTGGG*G*CAATAGCAATCATATCG-3′
D575A-F	5′-GTATTTTCTCGCTTTG*C*TGCATTAATTCTTGATGCTCGCTC-3′
D575A-R	5′-GAGCGAGCATCAAGAATTAATGCA*G*CAAAGCGAGAAAATAC-3′
D580A-F	5′-CTTTGATGCATTAATTCTTG*C*TGCTCGCTCCATTGCTTC-3′
D580A-R	5′-GAAGCAATGGAGCGAGCA*G*CAAGAATTAATGCATCAAAG-3′
P*angN-Xho*I	5′-*CTCGAG*GTTTCCTCATCAATCCAAAAGGTC-3′
P*angN-Pst*I	5′-*CTGCAG*CAACATGCAGCCTGCATTGGTGTTAATTC-3′
PEX-*angN*	5′-TGCCCATTATCTTTTCTTCC-3′
angN-T7L	5′-CGAAAGTTCTATTATTGATGTT-3′
angN-T7R	5′-ggatcctaatacgactcactatagggaggAGGTAATAAACTAACGGAGAAT-3′

[a] Restriction sites are underlined, base changed from the wt sequence are shown in italics, T7 promoter sequence in lower case

Cloning Kit (Invitrogen) resulting in the pMDL6 plasmid. A *Cla*I-*Bam*HI fragment was subcloned from pMDL6 into the *Cla*I-*Bam*HI sites of pBR325-M200 to generate the pMDL30 plasmid carrying the *angN* gene. After cloning in pBR325-M200 the entire *angN* gene was sequenced to verify that no mutation was generated in the *angN* gene during amplification or cloning. The pBR325-M200 cloning vector was derived from pBR325 by digestion with *Pst*I, blunting of the ends with T4 DNA polymerase (Gibco) and religation, resulting in a 4-bp deletion leading to the inactivation of the ampicillin resistance gene.

Site-directed mutagenesis

The plasmids pMDL6-D133A, pMDL6-D138A pMDL6-D575A and pMDL6-D580A were generated using the Quickchange™ site-directed mutagenesis kit (Stratagene), plasmid pMDL6 as a template and the primers listed in Table 2. The whole procedure was performed according to the manufacturer recommendations, with 16 cycles consisting of: 30 s at 95°C followed by 1 min at 55°C and 16 min at 68°C. Plasmids pMDL6-D133A/D575A and pMDL6-D138A/D580A were generated with the same procedure but using plasmids pMDL6-D133A and pMDL6-D138A as templates, respectively, and the appropriate primers. Site-specific mutations were confirmed by DNA sequencing. Once mutated, a *Cla*I-*Bam*HI fragment from each derivative was subcloned into the *Cla*I-*Bam*HI sites of pBR325-M200 to generate plasmids carrying the *angN* derivatives with mutations in the Cy domains listed in Table 1. Once cloned in pBR325-M200 the entire *angN* mutant genes were sequenced to verify that no other region of *angN* was affected during mutagenesis or cloning.

Construction of promoter fusions in pTL61T

Primers P*angN*-XhoI and P*angN*-PstI (Table 2) were used to amplify from pJM1 DNA a 350 bp fragment containing the 5′-end of the *angN* gene and the upstream region. The PCR product was cloned in the pCR®-BluntII-TOPO® vector using the Zero Blunt® TOPO® PCR Cloning Kit (Invitrogen) and subsequently subcloned into the *XhoI-PstI* sites of pTL61T to generate the pHNN-2 plasmid. The insert in pTL61T was sequenced to verify that the sequence of the PCR product is identical to the pJM1 sequence.

Growth in iron-limiting conditions and detection of anguibactin

For each mutant and wild type strain we determined the minimal inhibitory concentration (MIC) for EDDA by using liquid cultures at increasing concentrations of EDDA in M9 minimal medium at 25°C. From these analyses we chose a range of concentrations of EDDA to determine the ability of all the strains to grow in iron-limiting conditions.

The siderophore anguibactin was detected by CAS assay and by bioassays using strains CC9-16 and CC9-8 as previously described (Welch et al. 2000; Wertheimer et al. 1999) with few modifications. For the bioassay experiment each strain was grown in M9 minimal medium supplemented with 0.25 μM EDDA and after 16 h the culture volume corresponding to an $OD_{600\ nm} = 1$ was collected to obtain the supernatant. The supernatants were lyophilized to dryness, resuspended in 500 μl of methanol and stored at −80°C. Before spotting on the bioassay plates 10 μl of each sample were dried and resuspended in 3 μl of water.

Presence of anguibactin in the supernatant of strains grown in iron-limiting conditions was also determined by HPLC analysis. 100 μl aliquots from 1,000 fold concentrated supernatant were applied to HPLC (Beckmann Coulter System Gold) and the samples were analyzed on a ODS-AQ 120, 5 μm reversed-phase column C18, 150 mm length, 6 mm inner diameter (YMC, Waters). A binary gradient consisting of solvent A (0.01% trifluoracetic acid) and solvent B (100% acetonitrile and 0.01% trifluoracetic acid) was used: 1–26 min with 0–100% solvent B, 2 min 100% solvent B, 1 min 100–0% solvent B. Elution was carried out a room temperature with a flow rate of 1 ml/ min^{-1}. The column effluent was analyzed by monitoring the absorbance at 230 and 260 nm and fractions collected. Pools of 5 fractions (40 fractions were collected per sample, resulting in 8 pools per sample) were tested in bioassays using strains CC9-16 and CC9-8.

Fish infectivity assays

Virulence tests were carried out on juvenile rainbow trout (*Oncorhynchus mykiss*) weighing ca. 2.5–3 g, which were anesthetized with tricaine methane sulfonate (0.1 g/l). A total of 50 anesthetized fish were inoculated intramuscularly with 0.05 ml of each bacterial dilution, i.e., 50 fish per bacterial dilution. The dilutions were prepared with saline solution from 16 h cultures grown at 25°C in TSBS containing antibiotics for selection of the various plasmids harbored by the strains. The dilutions were prepared to test a range of cell concentrations from 10^1 to 10^7 cells/ml per strain. Therefore, 350 fish were tested per strain. After bacterial challenge, fish were maintained in fresh water at 13°C for 1 month and mortalities were checked daily. Virulence was quantified as the 50% lethal dose (LD_{50}) as determined by the method of Reed and Muench (Reed and Muench 1938).

β-Galactosidase assay

β-Galactosidase assays were performed as previously described (Miller 1972) on sodium dodecyl sulfate-chloroform-permeabilized cells grown in M9 medium supplemented with 0.5 μM EDDA (iron-limiting) and 4 μg/ml ferric ammonium citrate (iron rich). Cells grown in the iron-limiting medium were harvested after 12 h of growth at 25°C while for the iron rich medium the cells were harvested at 10 h. For all the strains, 1 ml of culture was used in the assay except for 775 pHNN-2 in iron-limiting conditions for which the assay was performed with 0.1 ml. The assays were repeated 4 times and each sample was tested in duplicate.

RNA isolation

A 1:100 inoculum from an overnight culture was grown in minimal medium with appropriate antibiotics. Cultures were grown with 2 μg/ml ferric ammonium citrate (iron rich) or with EDDA (iron-limiting) supplemented to achieve similar levels of iron-limiting stress for each strain tested (see figure legend). Total RNA was prepared when the culture reached an OD_{600} of 0.3–0.5 using the RNAwiz™ (Ambion) isolation kit, as previously described (Di Lorenzo et al. 2004).

Primer extension

Primer extension experiments were carried out with the synthetic primer PEX-*angN* (Table 2), which is complementary to the 5′-end region of the *angN* gene. The primer was end-labeled with T4-polynucleotide kinase (Life Technologies, Inc.) in the presence of [γ-^{32}P]-ATP and annealed to *V. anguillarum* 775 total RNA (50 μg). Reverse transcription from the primer by avian myeloblastosis virus reverse transcriptase (Promega) and separation on an urea-PAGE (6%) were carried out as previously described (Sambrook and Russell 2001). Manual sequencing was performed by the dideoxy chain-termination method using the Sequenase Version 2.0 DNA SequencingKit (USB), plasmid pMDL6 as template and the same primer used in the primer extension experiment.

Ribonuclease protection assays

Labeled riboprobes were generated by in vitro transcription of 1 μg of the linearized DNA with T7 or T3 RNA polymerase (MAXIscript® by Ambion) in the presence of [α-^{32}P]-UTP using as a template pSC50 (linearized with *Bam*HI) for *fatB* and pQSH6 (linearized with *Rsa*I) for *aroC*. The template DNA for the *angN* probe was generated by PCR using the two primers *angN*-T7L and *angN*-T7R in which the T7 promoter sequence was added at the 5′-end of the *angN*-T7R primer (Table 2). The probes were purified on a 6% polyacrylamide gel. For each probe, the amount corresponding to 4×10^5 cpm was mixed with each RNA sample (20 μg). Ribonuclease protection assays were performed using the RPA III™ (Ambion) kit following the supplier's instructions. The *aroC* riboprobe was used in each reaction as an internal control for the amount and quality of RNA.

Results

Analysis of the AngN sequence

We have reported the complete sequence of plasmid pJM1 and identified several *orfs* that encode predicted proteins that are part of the iron uptake system (Di Lorenzo et al. 2003). *orf10*, named *angN*, is predicted to encode a polypeptide (AngN) of 956 amino acids, with a calculated molecular mass of about 108 kDa (GenBank accession number NP943556 and Di Lorenzo et al. 2003). The predicted AngN amino acid sequence showed significant matches to members of the family of NRPSs such as VibF of *V. cholerae*, PchE and PchF of *Pseudomonas aeruginosa* and HMWP2 of *Yersinia pestis* (Butterton et al. 2000; Guilvout et al. 1993; Quadri et al. 1999). The similarity that AngN shares with these NRPSs is limited only to the cyclization (Cy) domain of these proteins. Like VibF but differently from the other proteins, the AngN protein possesses two tandem cyclization domains with 54% similarity and 35% identity to 927 amino acids at the N-terminal end of VibF.

Disruption of the *angN* gene and complementation with a wild type *angN* gene

To establish the role of this putative NRPS in anguibactin production, we selected from a collection of transposon insertions generated with Tn*3*::HoHo1 on a cloned region of pJM1, pJHC-T2612, two insertions, #120 and #68. These insertions occurred downstream of the iron transport-biosynthesis operon (Fig. 1) and each mutant was affected in anguibactin biosynthesis (Tolmasky et al. 1988). DNA sequencing of the #120 and #68 mutants proved that these insertions were in *angN* at 417 bp and 1,913 bp respectively from the 5′-end. Since the insertions were on pJHC-T2612 containing only a partial sequence of pJM1 (Fig. 1) we had to determine the effect of *angN* mutations on the iron-uptake system encoded by the whole pJM1 plasmid. Therefore, the Tn*3*::HoHo1 insertion in mutant #120 was integrated by allelic-exchange onto the pJM1 plasmid resulting in *V. anguillarum* 775(pJM1-120). As expected strain 775(pJM1-120) was unable to grow in iron-limiting conditions at increasing concentrations of the iron chelator EDDA since it did not produce anguibactin as detected by CAS (data not shown) and bioassay (Fig. 2a, b).

For complementation studies we constructed a clone, pMDL30, containing the complete *angN* gene (Fig. 1) expressed under the control of the tetracycline resistance gene promoter of the pBR325 vector and tested its ability to restore the growth of the *V. anguillarum* mutant 775(pJM1-120) under iron limitation. Plasmid pMDL30 was introduced into

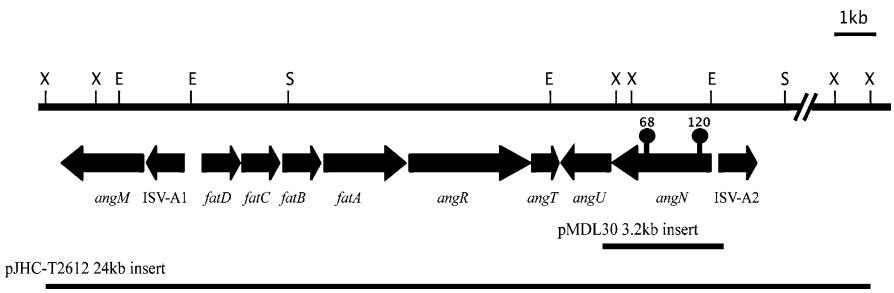

Fig. 1 Schematic of a 24 kb DNA region from the pJM1 plasmid encoding the *angN* gene and the iron transport-biosynthesis operon showing the site of Tn*3*::HoHo1 insertion in mutant #68 and #120. Restriction endonucleases: X, *Xho*I; E, *Eco*RI; S, *Sal*I

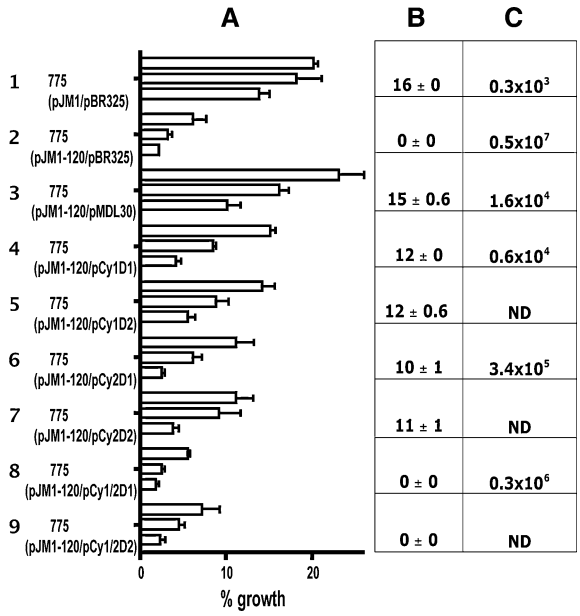

Fig. 2 Growth in iron-limiting conditions, anguibactin production and virulence of the *angN* mutant strains. (**a**) The ability of *V. anguillarum* strains to grow under-iron limitation is expressed as a percentage of the growth in EDDA normalized to the growth in iron rich conditions (4 μg/ml of ferric ammonium citrate) for each strain. Each column for each strain corresponds to concentrations of EDDA, from top to bottom, of 0.5, 0.75 and 1 μM, respectively. Results are the mean of three independent experiments with the error bars showing the standard error of the mean. (**b**) Measurement of anguibactin production by bioassay in mm of growth. The results shown are the average of three independent experiments with corresponding error. (**c**) Virulence experiments were carried out as described in Materials and methods and the LD_{50} values were calculated by the method of Reed and Muench (Reed and Muench 1938)

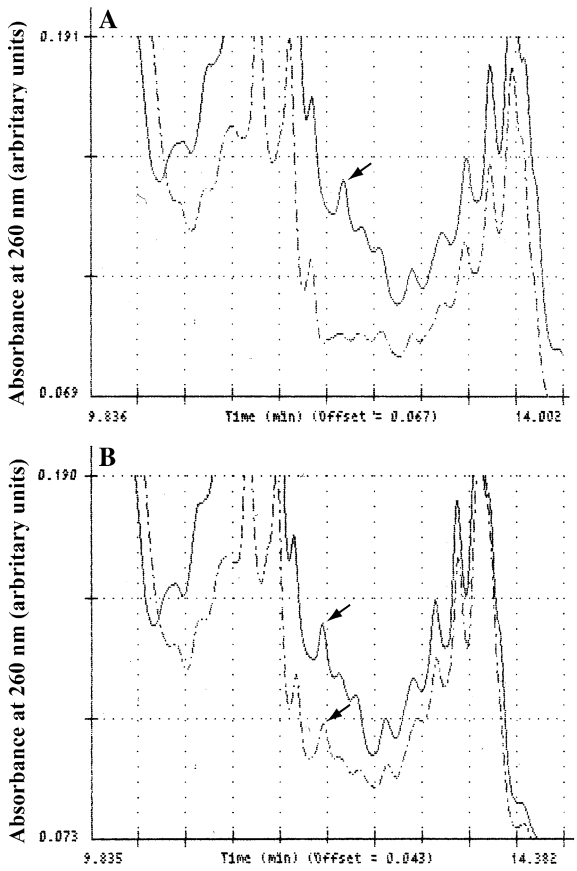

Fig. 3 HPLC profiles of supernatants from cultures of 775 and mutant derivatives. (**a**) Detail (from min 9.836 to min 14.002) of the HPLC profiles of supernatants from 775 (continuous line) and 775(pJM1#120), dashed line. The arrow points to the anguibactin peak. (**b**) Detail (from min 9.835 to min 14.382) of the HPLC profiles of supernatants from 775 (continuous line) and 775(pJM1#120/pMDL30), dashed line. The arrows point to the anguibactin peak. Shown are representative HPLC profiles

V. anguillarum 775(pJM1-120) and growth of the complemented mutant was determined in the presence of increasing concentrations of EDDA. The complemented strain grew as well as the wild type strain 775 under these conditions as seen by comparing growth of strains 1 and 3 in Fig. 2a. The fact that the *angN* gene was sufficient to restore growth of 775(pJM1-120) indicates that the insertion in mutant #120 was not polar to downstream genes.

The presence of anguibactin in the supernatant of strains 775, 775(pJM1-120) and 775(pJM1-120/pMDL30) grown in iron-limiting conditions was also determined by HPLC analysis using a reversed-phase C18 column and a binary gradient as described in the Materials and methods section. A peak identified as anguibactin by its retention time (12.06 min) and the UV spectra could be observed only in the wild type strain and in the 775(pJM1-120) mutant complemented with a wild type copy of the *angN* gene (Fig. 3). No peak corresponding to anguibactin was detected in strain 775(pJM1-120) confirming that a mutation affecting *angN* results in an anguibactin deficient phenotype (Fig. 3a). Pools of fractions collected from the HPLC column were tested in bioassay plates with strains CC9-16 and CC9-8 (the latter strain is used as a control for any iron contamination since it does not possess the anguibactin specific transport complex while strain CC9-16 can specifically transport anguibactin). Only the pools from strain 775 and 775(pJM1-120/pMDL30) containing the fraction of anguibactin allowed the

growth of strain CC9-16 and no growth was observed in the plates seeded with strain CC9-8 (data not shown).

Effect of site-directed modification of the *angN* gene on anguibactin production

It has been demonstrated that cyclization domains catalyze peptide bond formation and cyclization of amino acids such as threonine and cysteine (Duerfahrt et al. 2004; Marshall et al. 2002; Quadri et al. 1999). In the case of anguibactin it is likely that the thiazoline ring in anguibactin results from the incorporation of the amino acid cysteine in the siderophore. To determine the functionality of the two Cy domains of AngN in anguibactin biosynthesis, we performed site-directed mutagenesis of the first and second aspartic acid in the conserved Cy domain motif (DxxxxDxxS). Mutations in each of the aspartic acid residues within this motif have been shown to affect the activity of the Cy domains of VibF (Marshall et al. 2002). As shown in Fig. 4, both Cy domains of AngN possess the two aspartic acid residues in the Cy motif (**D**MIAI**D**PDS in Cy_1 and **D**ALIL**D**ARS in Cy_2). Each aspartic acid residue (shown as bold above) was mutated by site-directed mutagenesis to an alanine in the complementing construct pMDL30 generating four mutant constructs, pCy_1D_1-D133A, pCy_1D_2-D138A, pCy_2D_1-D575A and pCy_2D_2-D580A. Each plasmid was conjugated to the *angN*-deficient mutant 775(pJM1-120) and the resulting strains tested for their ability to grow in iron-limiting conditions. As shown in Fig. 2a, the insertion mutant #120 can still be complemented by the constructs harboring each of the mutated Cy domains (strains 4–7) although not as efficiently as with the construct harboring the wild type *angN* gene (strain 3). Furthermore, D to A mutations of each aspartic acid of the second cyclization domain seems to have a greater effect on the ability to complement the knock-out mutant. The growth in iron-limited medium of each strain correlates to their ability to produce anguibactin as determined by bioassays (Fig. 2b).

AngNCy1	**D**MIAI**D**PD**S**
AngNCy2	**D**ALIL**D**AR**S**
VibFCy1	**D**MIAC**D**AQ**S**
VibFCy2	**D**ALIV**D**GR**T**
PchECy	**D**LLAA**D**VE**S**
PchFCy	**D**FTLV**D**YA**S**
HMWP2Cy1	**D**LLIM**D**AS**S**
HMWP2Cy2	**D**NLLL**D**GL**S**

Fig. 4 Alignment of the conserved Cy motifs of AngN with the Cy motif found in other NRPSs. The conserved residues are shown in bold

Since a mutation in each of the aspartic acids had only a minor effect in anguibactin biosynthesis and growth, we decided to generate double mutations of the two Cy domains. Two plasmid derivatives of pMDL30 were constructed in which the first or the second aspartic acid of each domain, were mutated to an alanine ($pCy_{1/2}D_1$-D133A/D575A and $pCy_{1/2}D_2$-D138A/D580A). These two constructs were no longer able to complement the AngN-deficient mutant on pJM1 and no anguibactin could be detected by bioassay (Fig. 2a, b; strains 8 and 9).

AngN cyclization domains and anguibactin production in vivo

Our laboratory has shown that a clear correlation exists between anguibactin production and the multiplication of the bacterium in the fish host (Crosa et al. 1980; Di Lorenzo et al. 2004; Wertheimer et al. 1999). Since the mutations in *angN* affected anguibactin production (Fig. 2b), we wanted to determine how this would be reflected in the virulence phenotype of each strain. Experimental infections of rainbow trout were performed with several dilutions of the wild type and the 775(pJM1-120) mutant and this mutant complemented by the constructs harboring wild type or mutant *angN* to calculate the LD_{50} (Reed and Muench 1938). As expected mutations that resulted in an anguibactin-deficient phenotype (#120 insertion and #120 insertion complemented with the double aspartic acid mutant) had a reduced LD_{50} as compared to any strain that still produced anguibactin (Fig. 2c). Interestingly the LD_{50} for the mutant in the first Cy domain was of the same order of magnitude as the LD_{50} obtained with strain 775(pJM1-120) complemented with the wild type gene (Fig. 2c, strains 3 and 4), while the LD_{50} for the Cy_2 mutant strain was reduced by one order of magnitude as compared with the two strains above (Fig. 2c, strains 3, 4 and 6).

Transcription and regulation of the *angN* gene

The location of the promoter for the *angN* gene was determined by transcriptional fusion of the region upstream of *angN* with a promoterless *lacZ* gene. As described in the Materials and Methods section, a 350 bp fragment encompassing the 3′-end of the gene was cloned upstream of the *lacZ* gene in pTL61T, obtaining plasmid pHNN2. This construct was conjugated in strain 775 by triparental mating and the resulting strain was tested for *β*-galactosidase activity. The construct showed high activity in iron-limiting conditions (0.5 μM EDDA) while in iron rich conditions the Miller units measured were comparable to those of the empty vector control strain (Fig. 5a).

To determine the transcription start site of the *angN* mRNA, primer extension analysis was performed using primer PEX-*angN* complementary to the 5′-end of the *angN* gene and RNAs isolated from cultures grown at increasing iron limitation. Two iron-regulated products can be identified upstream of the *angN* gene (Fig. 5b, P1 and P2) with the first putative transcription start site 143 nt upstream of the start codon. Both transcription start sites fall within the region identified by *β*-galactosidase assay as the promoter region.

From these experiments it can be gathered that expression of the *angN* gene is repressed in iron rich conditions. To confirm this result we performed ribonuclease protection assays with total RNAs obtained from strain 775 cultures grown in iron rich (minimal medium supplemented with 2 μg/ml of ferric ammonium citrate) and in iron-limiting conditions (minimal medium supplemented with 0.5 μM EDDA and 1.5 μM EDDA). The ribonuclease protection results (Fig. 6 panel a, lanes 1 and 2) clearly show that *angN* mRNA is virtually undetected in iron

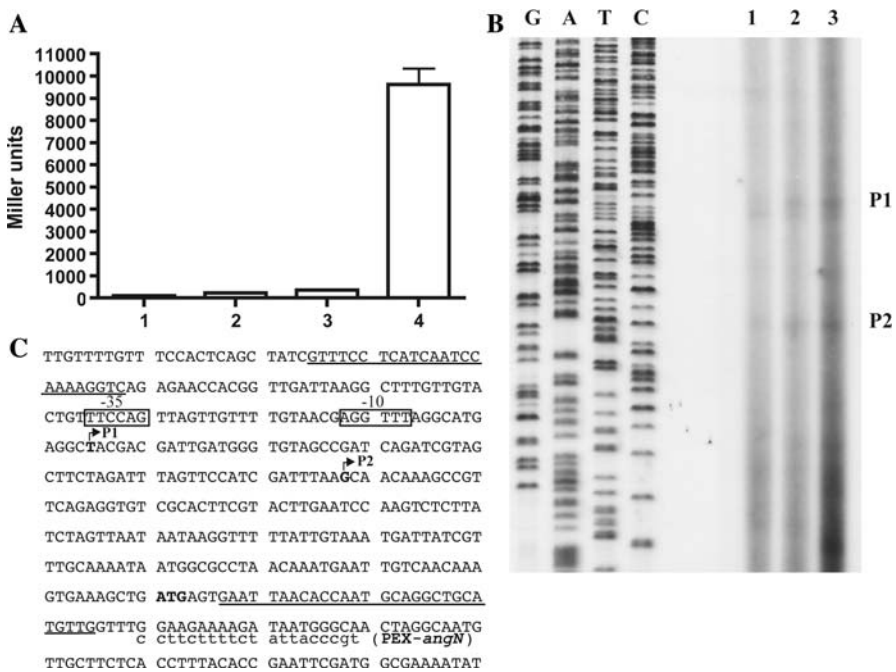

Fig. 5 Mapping of *angN* promoter and the transcription start sites of *angN* mRNA. (**a**) *β*-galactosidase assays with *V. anguillarum* strains (lanes 1 and 2, 775 pTL61T; lanes 3 and 4 775 pHNN-2) grown in iron rich (lanes 1 and 3, 4 μg/ml ferric ammonium citrate) or in iron-limiting (lanes 2 and 4, 0.5 μM EDDA) conditions. (**b**) Primer extension analysis using a primer complementary to the 5′-end of the *angN* gene and RNA obtained from cultures grown in iron rich (lane 1, 2 μg/ml ferric ammonium citrate) and in iron-limiting conditions (lane 2, 1.5 μM EDDA; lane 3, 2 μM EDDA). Lanes G, A, C and T represent the sequence of plasmid pMDL6 using primer PEX-*angN*. P1 and P2 are putative transcription start sites for the *angN* gene. (**c**) The nucleotide sequence of the region upstream of the *angN* gene is shown with the primer used in the primer extension experiment and the location of the putative transcription starts (arrowheads P1 and P2 and bold letters). The −35 and −10 sequences for the P1 product are shown as open boxes and the ATG for AngN is in bold. The sequences corresponding to the primers used to construct the *lacZ*-fusion are underlined

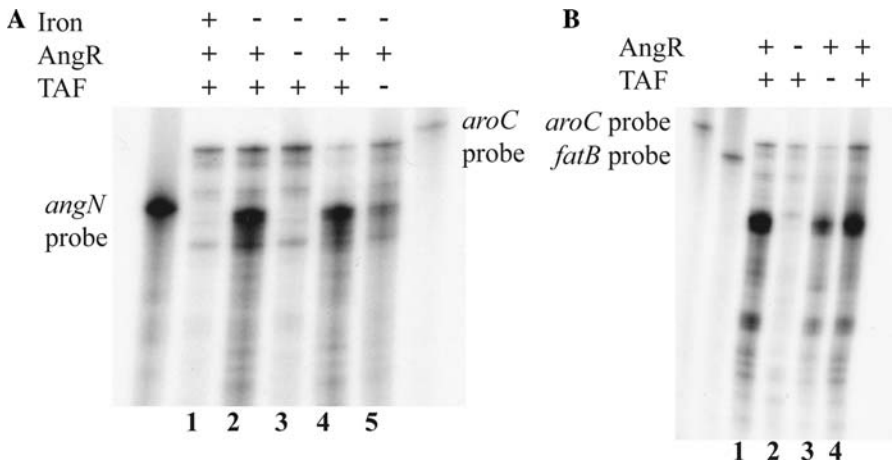

Fig. 6 Effect of iron, AngR and TAF on transcription of *angN* and *fatB*. (**a**) Ribonuclease protection assay using a probe specific for the *angN* gene and total RNA isolated from cultures grown under iron rich and iron-limiting conditions. *V. anguillarum* wild type (lanes 1, 2 and 4); *V. anguillarum* AngR-deficient strain (lane 3); *V. anguillarum* TAF-deficient strain (lane 5). RNA obtained under: iron rich conditions, lane 1 (2 μg/ml ferric ammonium citrate); iron-limiting conditions, lanes 2 and 4 (1.5 μM EDDA) and lanes 3 and 5 (0.5 μM EDDA). (**b**) Ribonuclease protection assay with the same RNA used in panel (**a**) from the cultures grown under iron-limiting conditions using a *fatB*-specific riboprobe. *V. anguillarum* wild type (lanes 1 and 4); *V. anguillarum* AngR-deficient strain (lane 2); *V. anguillarum* TAF-deficient strain (lane 3). The *aroC*-specific riboprobe is included in both Ribonuclease protection assays to provide an internal control for the quality of the RNA and the amount of RNA loaded onto the gel, since the *aroC* gene is expressed independently of the iron concentration of the cell

rich conditions, while *angN* is highly transcribed in iron-limiting conditions. A riboprobe specific for the *aroC*-mRNA was added to each reaction as a control for RNA quality and loading.

In the anguibactin-mediated iron uptake system two positive regulators, AngR and TAF, have been identified that regulate expression of genes included in the iron transport-biosynthesis operon, *fatDCBAangRT* (Chen et al. 1996; Wertheimer et al. 1999). Since the *angN* promoter is adjacent to an ISVA2-transposase gene and transcribed in the opposite orientation, mirroring the organization of the promoters of the *fatDCBAangRT* and the *tnp-angM* operons (Di Lorenzo et al. 2004), we wished to determine whether AngR and/or TAF products also regulate the transcription of *angN*. RNA was extracted from cultures of $angR^{-}taf^{+}$ and $angR^{+}taf^{-}$ strains that were grown in iron-limiting conditions (minimal medium supplemented with 0.5 μM EDDA) and the Ribonuclease protection assay was performed using an *angN* specific probe. We compared the changes in expression of the *angN*-mRNA and the *fatDCBAangRT* mRNA using a *fatB*-specific probe. Figure 6 shows that AngR and TAF have a similar effect on expression of *angN* (panel a, lanes 3 and 5) as of *fatB* (panel b, lanes 2 and 3) demonstrating that in addition to the iron transport-biosynthesis operon promoter they can also enhance transcription from the *angN* promoter.

Discussion

Sequencing of the plasmid pJM1 of *V. anguillarum* resulted in the identification of several genes encoding NRPSs and tailoring enzymes (Di Lorenzo et al. 2003). In this work we have characterized one of these genes, *angN*, and established its role in vivo in anguibactin production and in virulence.

As part of this analysis we found that the predicted AngN protein showed homology with the cyclization domain of other NRPSs. AngN consists of two Cy domains in tandem with no associated additional domains and it is the first NRPS so far identified that has two free-standing Cy domains. Each domain has the two aspartic acids residues in the highly conserved motif that have been shown in in vitro experiments with VibF to be essential for the function of Cy domains (Marshall et al. 2002). In this work we have shown that single amino acid substitutions of the conserved aspartic acid in either one of the domains

partially abolishes anguibactin production, suggesting the possibility that one wild type Cy domain of AngN is sufficient to catalyze the cyclization reaction. Furthermore, mutations in the aspartic acid residues of both Cy domains (D133A/D575A and D138A/D580A) resulted in cessation of anguibactin biosynthesis demonstrating that these Cy domains are essential for production of anguibactin in vivo. Using HPLC analysis we showed that anguibactin can be detected only in supernatants from strains in which an active AngN is present. We also confirmed that the bioassay with strain CC9-16 is specific for anguibactin, since only the pools containing the anguibactin fraction resulted in growth of this strain.

It is of interest that AngR, which plays a role in regulation of the expression of iron transport genes as well as in the production of anguibactin, possesses also a cyclization (Cy) domain (Wertheimer et al. 1999). However the first aspartic acid residue of the conserved motif is replaced by an asparagine in the Cy domain of AngR. From the results presented in this work the Cy domain of AngR is unable to functionally replace the mutated Cy domains of AngN in anguibactin production. Therefore, an attractive possibility is that AngR provides the adenylation domain required to activate cysteine, prior to tethering it on the peptidyl carrier protein domain of AngM while either of the Cy domains of AngN is in charge of the condensation step between DHBA and cysteine (Fig. 7).

The unusual domain arrangement of AngN and the results obtained with the mutants affecting only one domain of AngN suggest that AngN is a protein with a redundant catalytic activity, in which each domain is functional independently of the other. However, the differences in the LD_{50} of the mutants in the virulence experiments suggest that only an AngN protein with two functional Cy domains results in the most efficient synthesis of anguibactin in vivo.

It is intriguing that a division of labor by two Cy domains was demonstrated in an in vitro experiment with VibF (Marshall et al. 2002), an NRPS that in addition to two cyclization domains also has an adenylation, a peptidyl carrier protein and two condensation domains, and thus is not a free standing cyclization enzyme like AngN. From the experiments with VibF it was proposed that the first cyclization domain does the actual cyclization reaction while the second one does the condensation step (Marshall

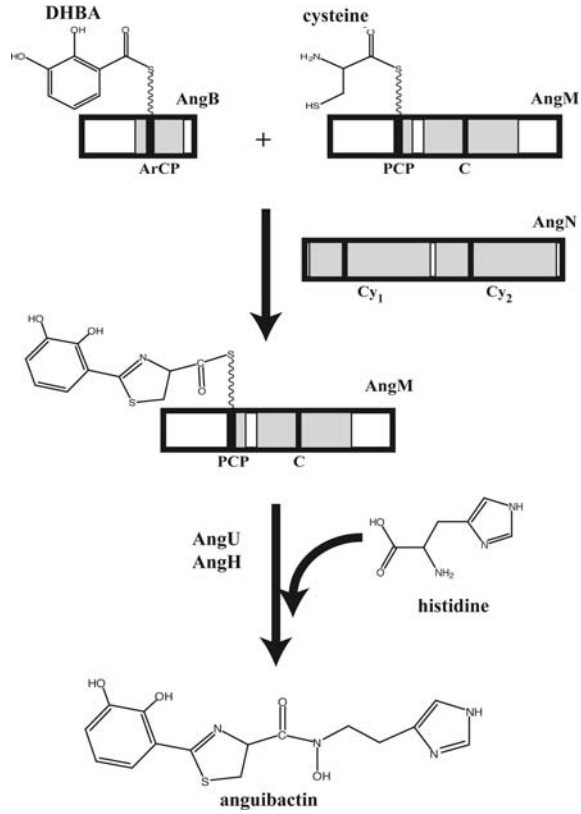

Fig. 7 Model of the biosynthetic step catalyzed by AngN. The Cy domains of AngN catalyze peptide bond formation and cyclization between DHBA loaded on the ArCP domain of AngB and cysteine tethered onto the PCP domain of AngM. AngU and AngH are tailoring enzymes that convert histidine to hydroxyhistamine

et al. 2002). Sequence alignment of each Cy domain of AngN with other seven Cy domains ($VibFCy_1$, $VibFCy_2$, $HMWP2Cy_1$, $HMWP2Cy_2$, PchFCy, PchECy and the other Cy domain of AngN) revealed an average of 22.7% identity for Cy_1 and 18.6% identity for Cy_2. The percentage of identity of $AngNCy_2$ to each one of the other Cy domains is relatively lower than the overall average of 25.4% of the other domains while the similarity shared with $VibFCy_2$ is significantly higher (32%). Furthermore, the amino acid residues that have been shown to be important in cyclization but not in condensation activity of Cy domains (Duerfahrt et al. 2004) were not conserved in the Cy_2 domain of AngN and in the Cy_2 domain of VibF. However, we cannot conclude from our in vivo results with the AngN mutants that the division of labor observed in VibF Cy domains occurs also in AngN domains since site-directed mutations in either

Cy_1 or Cy_2 are still proficient in anguibactin production.

In this work we also determined that expression of the *angN* gene is negatively regulated by the iron concentration of the culture medium. Analysis of the sequence at the *angN* promoter shows that it overlaps a putative transposase promoter that transcribes in the opposite direction, thus mirroring the situation described for the *tnp-angM* and iron transport-biosynthesis promoters (Di Lorenzo et al. 2004). An exciting result was that the *angN* promoter is positively regulated by AngR and TAF, making it another member of the AngR and TAF regulon.

Acknowledgments This project was supported by Grants from the National Institute of Health, AI19018 and GM64600, to J.H.C. We are grateful to Christopher T. Walsh for his insightful discussions.

References

Actis LA, Fish W, Crosa JH et al (1986) Characterization of anguibactin, a novel siderophore from *Vibrio anguillarum* 775(pJM1). J Bacteriol 167:57–65

Actis LA, Tolmasky ME, Farrell DH et al (1988) Genetic and molecular characterization of essential components of the *Vibrio anguillarum* plasmid-mediated iron-transport system. J Biol Chem 263:2853–2860

Actis LA, Tolmasky ME, Crosa JH (1999) Vibriosis. In: Woo P, Bruno D (eds) Fish diseases and disorders Viral, bacterials and fungal infections. Cab International Publishing, Wallingford, pp 523–557

Alice AF, Lopez CS, Crosa JH (2005) Plasmid- and chromosome-encoded redundant and specific functions are involved in biosynthesis of the siderophore anguibactin in *Vibrio anguillarum* 775: a case of chance and necessity? J Bacteriol 187:2209–2214. doi:10.1128/JB.187.6.2209-2214.2005

Altschul SF, Gish W, Miller W et al (1990) Basic local alignment search tool. J Mol Biol 215:403–410

Birnboim HC, Doly J (1979) A rapid alkaline extraction procedure for screening recombinant plasmid DNA. Nucleic Acids Res 7:1513–1523. doi:10.1093/nar/7.6.1513

Bolivar F (1978) Construction and characterization of new cloning vehicles. III. Derivatives of plasmid pBR322 carrying unique *Eco* RI sites for selection of *Eco* RI generated recombinant DNA molecules. Gene 4:121–136. doi:10.1016/0378-1119(78)90025-2

Boyer HW, Roulland-Dussoix D (1969) A complementation analysis of the restriction and modification of DNA in *Escherichia coli*. J Mol Biol 41:459–472. doi:10.1016/0022-2836(69)90288-5

Braun V, Killmann H (1999) Bacterial solutions to the iron-supply problem. Trends Biochem Sci 24:104–109. doi:10.1016/S0968-0004(99)01359-6

Butterton JR, Choi MH, Watnick PI et al (2000) *Vibrio cholerae* VibF is required for vibriobactin synthesis and is a member of the family of nonribosomal peptide synthetases. J Bacteriol 182:1731–1738. doi:10.1128/JB.182.6.1731-1738.2000

Chen Q, Wertheimer AM, Tolmasky ME et al (1996) The AngR protein and the siderophore anguibactin positively regulate the expression of iron-transport genes in *Vibrio anguillarum*. Mol Microbiol 22:127–134. doi:10.1111/j.1365-2958.1996.tb02662.x

Crosa JH, Hodges LL, Schiewe MH (1980) Curing of a plasmid is correlated with an attenuation of virulence in the marine fish pathogen *Vibrio anguillarum*. Infect Immun 27:897–902

Crosa JH, Walsh CT (2002) Genetics and assembly line enzymology of siderophore biosynthesis in bacteria. Microbiol Mol Biol Rev 66:223–249. doi:10.1128/MMBR.66.2.223-249.2002

Di Lorenzo M, Stork M, Tolmasky ME et al (2003) Complete sequence of virulence plasmid pJM1 from the marine fish pathogen *Vibrio anguillarum* strain 775. J Bacteriol 185:5822–5830. doi:10.1128/JB.185.19.5822-5830.2003

Di Lorenzo M, Poppelaars S, Stork M et al (2004) A nonribosomal peptide synthetase with a novel domain organization is essential for siderophore biosynthesis in *Vibrio anguillarum*. J Bacteriol 186:7327–7336. doi:10.1128/JB.186.21.7327-7336.2004

Duerfahrt T, Eppelmann K, Muller R et al (2004) Rational design of a bimodular model system for the investigation of heterocyclization in nonribosomal peptide biosynthesis. Chem Biol 11:261–271. doi:10.1016/S1074-5521(04)00024-9

Figurski DH, Helinski DR (1979) Replication of an origin-containing derivative of plasmid RK2 dependent on a plasmid function provided in trans. Proc Natl Acad Sci USA 76:1648–1652. doi:10.1073/pnas.76.4.1648

Finking R, Marahiel MA (2004) Biosynthesis of nonribosomal peptides1. Annu Rev Microbiol 58:453–488. doi:10.1146/annurev.micro.58.030603.123615

Fischbach MA, Walsh CT (2006) Assembly-line enzymology for polyketide and nonribosomal peptide antibiotics: logic, machinery, and mechanisms. Chem Rev 106:3468–3496. doi:10.1021/cr0503097

Guilvout I, Mercereau-Puijalon O, Bonnefoy S et al (1993) High-molecular-weight protein 2 of *Yersinia enterocolitica* is homologous to AngR of *Vibrio anguillarum* and belongs to a family of proteins involved in nonribosomal peptide synthesis. J Bacteriol 175:5488–5504

Hirsch PR, Beringer JE (1984) A physical map of pPH1JI and pJB4JI. Plasmid 12:139–141. doi:10.1016/0147-619X(84)90059-3

Keating TA, Walsh CT (1999) Initiation, elongation, and termination strategies in polyketide and polypeptide antibiotic biosynthesis. Curr Opin Chem Biol 3:598–606. doi:10.1016/S1367-5931(99)00015-0

Linn T, St Pierre R (1990) Improved vector system for constructing transcriptional fusions that ensures independent translation of *lacZ*. J Bacteriol 172:1077–1084

Marahiel MA, Stachelhaus T, Mootz HD (1997) Modular peptide synthetases involved in nonribosomal peptide

synthesis. Chem Rev 97:2651–2674. doi:10.1021/cr960029e

Marshall CG, Burkart MD, Keating TA et al (2001) Heterocycle formation in vibriobactin biosynthesis: alternative substrate utilization and identification of a condensed intermediate. Biochemistry 40:10655–10663. doi:10.1021/bi010937s

Marshall CG, Hillson NJ, Walsh CT (2002) Catalytic mapping of the vibriobactin biosynthetic enzyme VibF. Biochemistry 41:244–250. doi:10.1021/bi011852u

Miethke M, Marahiel MA (2007) Siderophore-based iron acquisition and pathogen control. Microbiol Mol Biol Rev 71:413–451. doi:10.1128/MMBR.00012-07

Miller J (1972) Experiments in molecular genetics. Cold Spring Harbor, NY

Miller DA, Walsh CT (2001) Yersiniabactin synthetase: probing the recognition of carrier protein domains by the catalytic heterocyclization domains, Cy1 and Cy2, in the chain-initiating HWMP2 subunit. Biochemistry 40:5313–5321. doi:10.1021/bi002905v

Naka H, Lopez CS, Crosa JH (2008) Reactivation of the vanchrobactin siderophore system of *Vibrio anguillarum* by removal of a chromosomal insertion sequence originated in plasmid pJM1 encoding the anguibactin siderophore system. Environ Microbiol 10:265–277

Quadri LE, Keating TA, Patel HM et al (1999) Assembly of the *Pseudomonas aeruginosa* nonribosomal peptide siderophore pyochelin: In vitro reconstitution of aryl-4, 2-bisthiazoline synthetase activity from PchD, PchE, and PchF. Biochemistry 38:14941–14954. doi:10.1021/bi991787c

Ratledge C (2007) Iron metabolism and infection. Food Nutr Bull 28:S515–S523

Reed LJ, Muench H (1938) A simple method of estimating fifty per cent endpoints. Am J Hyg 27:493–497

Sambrook J, Russell DW (2001) Molecular cloning: a laboratory manual, vol 3rd. Cold Spring Harbor Laboratory Press, Cold Spring Harbor, NY

Tolmasky ME, Actis LA, Crosa JH (1988) Genetic analysis of the iron uptake region of the *Vibrio anguillarum* plasmid pJM1: molecular cloning of genetic determinants encoding a novel trans activator of siderophore biosynthesis. J Bacteriol 170:1913–1919

von Dohren H, Dieckmann R, Pavela-Vrancic M (1999) The nonribosomal code. Chem Biol 6:R273–R279. doi:10.1016/S1074-5521(00)80014-9

Walsh CT (2004) Polyketide and nonribosomal peptide antibiotics: modularity and versatility. Science 303:1805–1810. doi:10.1126/science.1094318

Walsh CT, Chen H, Keating TA et al (2001) Tailoring enzymes that modify nonribosomal peptides during and after chain elongation on NRPS assembly lines. Curr Opin Chem Biol 5:525–534. doi:10.1016/S1367-5931(00)00235-0

Walter MA, Potter SA, Crosa JH (1983) Iron uptake system mediated by *Vibrio anguillarum* plasmid pJM1. J Bacteriol 156:880–887

Wandersman C, Delepelaire P (2004) Bacterial iron sources: from siderophores to hemophores. Annu Rev Microbiol 58:611–647. doi:10.1146/annurev.micro.58.030603.123811

Welch TJ, Chai S, Crosa JH (2000) The overlapping *angB* and *angG* genes are encoded within the trans-acting factor region of the virulence plasmid in *Vibrio anguillarum*: essential role in siderophore biosynthesis. J Bacteriol 182:6762–6773. doi:10.1128/JB.182.23.6762-6773.2000

Wertheimer AM, Verweij W, Chen Q et al (1999) Characterization of the *angR* gene of *Vibrio anguillarum*: essential role in virulence. Infect Immun 67:6496–6509